LBL-6686

RECEIVED
LAWRENCE
BERKELEY LABORATORY

MAR 8 1978

LIBRARY AND
DOCUMENTS SECTION

A COMPARISON OF THE MICROSTRUCTURE AND MECHANICAL PROPERTIES OF 300-M STEEL MANUFACTURED BY THE VACUUM ARC REMELT AND THE ELECTROSLAG REMELT PROCESSES

Thomas A. Lechtenberg
(M. S. thesis)

September 1977

Prepared for the U. S. Department of Energy
under Contract W-7405-ENG-48

TWO-WEEK LOAN COPY

This is a Library Circulating Copy
which may be borrowed for two weeks.
For a personal retention copy, call
Tech. Info. Division, Ext. 5716

LAWRENCE BERKELEY LABORATORY
UNIVERSITY OF CALIFORNIA
BERKELEY

LBL-6686

LEGAL NOTICE

This report was prepared as an account of work sponsored by the United States Government. Neither the United States nor the Department of Energy, nor any of their employees, nor any of their contractors, subcontractors, or their employees, makes any warranty, express or implied, or assumes any legal liability or responsibility for the accuracy, completeness or usefulness of any information, apparatus, product or process disclosed, or represents that its use would not infringe privately owned rights.

A COMPARISON OF THE MICROSTRUCTURE AND MECHANICAL PROPERTIES OF 300-M STEEL MANUFACTURED BY THE VACUUM ARC REMELT AND THE ELECTROSLAG REMELT PROCESSES

Contents

Abstract v

I. Introduction 1

II. Experimental 4

1. Material Preparation 4

2. Heat Treatment 4

3. Mechanical Testing 5

A. Tensile Properties 5

B. Fracture Toughness (K_{IC}) Testing 5

C. Charpy Impact Testing 6

4. X-Ray Analysis 6

5. Optical Metallography 6

6. Scanning Electron Microscopy and Energy Dispersive Analysis of X-Rays 7

III. Results 8

1. Selection of Heat Treatments 8

2. Ingot Cleanliness 8

3. Mechanical Behavior 9

A. Tensile Properties 9

B. Fracture Toughness, K_{IC} 9

C. Charpy Impact Energy 9

4. Retained Austenite 10

A. Fracture Surface Morphology 10

5. Microstructural Characterization 10

IV. Discussion 12

1. The Effect of Reduced Impurities 12

2. The Effect of Variation in Inclusion Contents 14

V. Conclusions 17

Acknowledgements 18

References 19

Tables 21

Figure Captions 25

Figures 27

A COMPARISON OF THE MICROSTRUCTURE AND MECHANICAL PROPERTIES OF 300-M STEEL MANUFACTURED BY THE VACUUM ARC REMELT AND THE ELECTROSLAG REMELT PROCESSES

Thomas A. Lechtenberg

Materials and Molecular Research Division
Lawrence Berkeley Laboratory
and
Department of Materials Science and Engineering
University of California
Berkeley, California 94720

Abstract

The transverse (T-L) and longitudinal (L-T) mechanical properties of Electroslag Refined (ESR) and Vacuum Arc Remelt (VAR) 300-M steel were measured. These were related to the microstructural and chemical differences which resulted from the two melting processes. It was found that the ESR process resulted in a cleaner steel. Impurity elements were reduced and inclusions were finer and more evenly dispersed. The Charpy impact energies of the ESR steel were nearly doubled those of the VAR. Also the fracture toughness of the ESR 300-M showed no temper embrittlement in the 350 to 500°C tempering range whereas that of the VAR material did.

I. INTRODUCTION

The increasing demands of the aerospace industry and the military for improved performance, especially in terms of toughness, in materials of high strength has lead to the investigations of melting and casting processes which result in clean steels.[1,2] One such process, the electroslag refining (ESR) technique, has been receiving increasing attention recently. The ESR process gives a steel low in impurities such as sulphur[3-6] and also reduces the size of non-metallic inclusions.[7] The improvement in cleanliness is expected to result in an increase in toughness of the steel. An objective of this study was to characterize the mechanical properties of an ultrahigh strength steel manufactured by two different processes, namely the ESR process and the vacuum arc remelt (VAR) process.

An increase in yield strength of a steel is generally associated with a decrease in toughness.[8,9] However, it has been demonstrated that, through control of metallurgical and microstructural variables, an increase in fracture toughness without a significant decrease in yield strength is possible.[10] Among the microstructural features which affect toughness are the nature of the martensitic structure (dislocated vs twinned),[11,12] retained austenite at lath boundaries,[10] the size of the grains[13,14] and the presence of phases such as primary ferrite which leads to so called duplex microstructures.[15] These microstructural features can be controlled by heat treatments. Also it has been reported that the cleanliness of a steel can significantly affect its mechanical properties. The ESR process has been shown

to decrease inclusion size and volume fraction and distribute the remaining inclusions more evenly.

The ESR process is a secondary refining process where a consumable electrode is melted such that droplets of molten metal pass through a refining slag layer which is usually based on calcium fluoride (CaF_2) as the primary constituent and calcium oxide (CaO) to promote desulphurization. The ingot is continuously solidified in a water cooled mold. The process is illustrated in Fig. 1. This technique is particularly efficient in removing sulphur and through proper slag control, phosphorous can also be removed.[16] Due to the slag layer on the molten metal pool, ingot wall and the water cooled mold, vertical dendritic growth is promoted.[17,18] Casting defects such as shrinkage, axial porosity, ingot surface quality, and zonal segregation of elements are inhibited.[19,20]

The vacuum arc remelt (VAR) process is a secondary refining process and can also result in clean steels. However, conventional casting techniques have to be used which can result in coarse dendritic structures and other casting defects. The process is also expensive as compared to the ESR method. However, a significant amount of steel is made by the VAR process in this country and the mechanical properties of steels manufactured by this process have been characterized. In contrast the mechanical properties of ESR steels have not been fully characterized. It was of interest to characterize the properties of a steel manufactured by the ESR process and compare its properties of those of the equivalent steels manufactured by the VAR process.

The steel chosen was 300-M, a material known for potentially good strength-toughness combinations. Also the VAR 300-M has already been characterized to a great extent in other investigations.[21,22] Special attention was placed on the determination and comparison of transverse and longitudinal properties.

II. EXPERIMENTAL

1. Material Preparation

The VAR 300-M was obtained as commercial aircraft quality steel in the form of a 4 in. x 4 in. billet that had been forged and then homogenized. Part of the billet was cut and forged to 1 in. thick plate. Specimens for the longitudinal and transverse direction were cut from the forged plate. Figure 2(a) shows the orientation of the compact tension specimens with respect to the rolling direction.

The ESR 300-M was provided by the Army Materials and Mechanics Research Center. The ingot was produced as a 300 lb heat which was annealed at 1300°C for 24 hr, forged and flame cut to a reasonable size for shipping. Specimens were cut from the forged plate.

The chemical compositions of the VAR and ESR 300-M are given in Table 1.

2. Heat Treatment

Heat treatments were carried out on rough machined fracture toughness, round and flat tensile, and Charpy V-Notch specimens. The heat treatments consisted of (1) austenitization at 900°C for 1 hr, suspended in a vertical tube furnace in an argon atmosphere (Fig. 2(b)),(2) quenching in agitated oil, and (3) tempering for 1 hr at various temperatures up to 600°C in molten salt baths followed by air cooling to room temperature.

3. Mechanical Testing*

A. Tensile properties

Room temperature longitudinal tensile properties were determined using ASTM specified round tensile specimens and also non-standard flat tensile specimens. Sketches of the specimens with pertinent details are shown in Fig. 3. The round tensile specimens were tested on the 300,000 lb MTS testing system at a constant loading rate of 0.05 cm/min. The flat tensile specimens were pulled on a 5000 kg capacity Instron machine at the same rate. Yield strengths were determined using the 0.2% strain offset from the load vs crosshead displacement curves. Elongation and reduction in area were found using the round tensile specimens only because the small cross sectional area of the flat tensile specimens resulted in variability of the area measurements.

B. Fracture toughness (K_{IC}) testing

Room temperature longitudinal and transverse plane strain fracture toughness values were determined using ASTM specified[23] compact tension specimens. These are shown in Fig. 4. All specimens were machined with the slot from the 1 in. thick ESR plate or the VAR billet described in the proceeding section. They were then heat treated and ground to specifications. A 0.008 in. wide slot was cut with an abrasive wheel to facilitate the introduction of the fatigue crack.

* Three tests per data point unless otherwise noted.

Precracking was done using a 300,000 lb capacity MTS testing machine at 8 cycles per second. Crack lengths were within ASTM specifications and the displacement was monitored with a crack opening displacement (COD) strain gage.

C. Charpy impact testing

Charpy blanks were heat treated, ground to dimensions, and the notch inserted. This is shown in Fig. 5. All tests were conducted at room temperature. VAR longitudinal Charpy data were compiled from work done at this laboratory[22,24] and by the author where verification and more data were required.

4. X-Ray Analysis

Volume percentage of retained austenite was determined with an X-Ray Diffraction unit using procedures described elsewhere,[25] and by the magnetic saturation technique.[26] X-ray analysis on the diffractometer used specimens cut from the center of the compact tension specimens; these were ground on successively finer papers and polished at 1 μ, then etched in 100 m H_2O_2 + 5 m HF solution for 5 min, then repolished lightly on a 1μ diamond paste. The etching was done to remove disturbed metal.

5. Optical Metallography

Samples for optical metallography were obtained from the compact tension specimens. These were mounted in bakelite, ground on successively finer papers to 600 grit, and polished on the 6μ and 1μ diamond paste wheel. The material was etched with a 2% nital solution to reveal the microstructures. Banding of the VAR material was seen

using the same nital etchant. The ASTM grain size was determined by comparison to standard plates.

6. Scanning Electron Microscopy and Energy Dispersive Analysis of X-Rays

An AMR scanning electron microscope at 20 kV was used to examine the fracture surfaces of the compact tension specimens and Charpy bars.

An energy dispersive analysis of x-rays attachment was mounted on the microscope and used to analyze the artifacts found on the fracture surfaces. The analysis was facilitated by the use of a small computer which compared the dispersed x-rays to known standards on preprogammed tapes.

III. RESULTS

1. Selection of Heat Treatments

The mechanical properties and microstructure of normally cast and VAR 300-M has been well characterized in earlier investigations.[10,22] As the aim of this project was a direct comparison between the properties of VAR and ESR steel, the heat treatments selected were based on data available in the literature for the VAR steel. An austenitization temperature of 900°C was used, accompanied by a subsequent oil quench. Tempering was performed at various temperatures to 650°C.

2. Ingot Cleanliness

Specimens for optical examination were cut from the as-received VAR billet and the as-received ESR plate. After polishing and proper etching they were examined for evidence of banding. The microstructures are shown in Fig. 6 where in (a) banding in the VAR material was observed and in (b) a noticeable lack of banding was present in the ESR material. Specimens taken from three different sections of the ESR plate showed no significant banding through some banding was seen later in a few of the tempered specimens.

A metallographic examination for inclusions was also made on samples austenitized for 1 hr at 900°C and oil quenched. The results are shown in Fig. 7; Fig. 7(a) and (b) shows the ESR 300-M and VAR 300-M respectively after a 1μ diamond wheel polish. These inclusions in these samples were analyzed on the EDAX-SEM and were found to be MnS.

3. Mechanical Behavior

A. Tensile properties

Yield strength, ultimate tensile strength (UTS), percent reduction in area, and percent elongation are listed in Table 2. It was observed that the UTS valves were nearly the same for each process with similar heat treatments. The yield strengths also exhibited approximately the same behavior. Elongation and reduction in area are graphed in Fig. 8. The elongation for the VAR after tempering at 500°C showed a marked drop. This corresponds to the same temperature range where a drop in the K_{IC} was observed.

B. Fracture toughness, K_{IC}

Plane strain fracture toughness for the longitudinal and transverse rolling directions of both VAR and ESR 300-M were determined and the results are summarized in Table 3. The data are shown graphically in Figs. 9 and 10. It is shown in Fig. 9 that there was a marked difference in the longitudinal and transverse K_{IC} values at the same strength levels for the VAR 300-M. The longitudinal section exhibited higher K_{IC} values, the most pronounced difference being in the tempering temperature region of 350-450°C. Figure 10 displays the ESR longitudinal and transverse K_{IC}. There is little difference between the longitudinal and transverse K_{IC} values over the whole tempering range.

C. Charpy impact energy

The room temperature Charpy impact energy, C_V, data are given in Table 4 for the VAR and ESR material. The results are also shown in Fig. 11. There is a large difference in the energy absorbed associated with the two processes. The ESR 300-M in the transverse orientation

and C_V values 10 ft-lb higher in nearly all instances than those of the transverse VAR specimens. The ESR material also exhibited higher values of C_V in the longitudinal orientations.

There was a decrease in the C_V values in the 350 500°C tempering range. This was noticed in the ESR transverse and longitudinal and the VAR longitudinal orientations. The transverse VAR showed only a slight decrease from the peak toughness at 200°C. For all orientations there was a recovery of impact energies above 500°C.

4. Retained Austenite

The percent retained austenite as determined by the X-Ray Diffractometer is graphed in Fig. 12 for the VAR steel. The as-quenched condition had a high percent of retained austenite. As tempering occurred, increasing amounts transformed until at 500°C there was virtually 0° retained austenite present.

A. Fracture surface morphology

The fracture surfaces are shown in Fig. 13 for the VAR transverse sections. the fracture surfaces for the as-quenched, 200°C, and 300°C temper conditions displayed mostly dimple rupture and some quasi-cleavage. Following tempering at 400°C, the amount of quasi-cleavage increased, and following the 500°C temper, the fracture mode was predominately intergranular with some decohesion between grains. Note should be made of the "inclusion trail" in Fig. 13(a) labeled "AC."

5. Microstructural Characterization

The prior austenite grain size was determined to be ASTM No. 7 for both the VAR and ESR material. Since the same austenitization temperature was employed throughout the study only two determinations

were made. However, whenever possible the grain size was examined for deviation from this expected size and none was found.

Micrographs of the ESR 300-M are shown in Fig. 15. The microstructure was mostly martensitic in the as-quenched condition with a typical acicular structure. The 300°C and 400°C temper conditions show the tempered martensitic structure also. Figure 15(c) shows the 500°C temper condition where the precipitation of the Fe_3C has become pronounced. The microstructures observed for the VAR steel were nearly identical.

IV. DISCUSSION

Two of the most important process variables in the production of steel which affect the mechanical properties are ingot cleanliness and surface quality. Specifically chemical impurities and inclusions have a major impact. It has been known for some time that impurity elements such as S and P have an adverse effect on notch toughness. It is thought that S and P concentrate at the prior austenite grain boundaries as thin films which reduce the toughness by causing a loss of cohesion.[28,29] Also, dendritic microsegregation can lead to paths of easy crack propagation by causing a small region at dendrite interfaces across which the chemistry is inhomogeneous.[27] Inclusions can act as crack initiators due to the stress concentrations at the matrixinclusion interface[30] and the distribution of inclusions has been linked to the fracture toughness.[27]

1. The Effect of Reduced Impurities

Temper embrittlement occurs in quenched and tempered steels as they are slowly cooled through the 550°C to 370°C temperature range. The embrittlement is due to a loss of cohesion at the grain boundaries and is believed to be caused by the segregation of tramp impurity elements such as phosphorous to the grain boundaries during austenitization. These impurities precipitate when cooled through the temperature range mentioned above.[31-33] The ESR process significantly reduced the phosphorous content, from 0.012% (in the VAR steel) to 0.006%. The effect on the toughness is best illustrated in Fig. 16. The VAR material in the 350-550°C tempering range suffered a severe loss of toughness while the ESR steel did not. This is also shown in Fig. 8.

The VAR steel exhibited a decrease in the reduction of area in the same tempering range. The fracture surfaces of the transverse specimens show this same embrittling effect in the series of fractographs in Figs. 13 and 14. Figure 13 is of the VAR material and Fig. 14 is of the ESR material as it was tempered through the sequence of room temperature, 300, 400 and 500°C. The fracture surfaces of the as-quenched specimens showed primarily the dimple rupture mode with some cleavage. Dimples are the result of microvoid coalescence, i.e., the decohesion of particles in the matrix and the subsequent growth until one void joins another. Where no particle was observed in a dimple it could have been formed around a small carbide which was either too small to be detected, or removed during sample preparation. The VAR material in the as-quenched condition (Fig. 13(a)) showed some evidence of void formation around a MnS particle. The inclusion stringer is labeled "AC." It is seen that a large MnS particle sits in the void that formed around it. Generally, the VAR material exhibited a coarser dimple rupture structure than the ESR steel for the same as-quenched condition (Fig. 14(a)). The ESR shows fine dimples with some quasi-cleavage. These finer dimples are associated with fewer and finer inclusions and carbides.

The fracture surfaces in the 300°C temper condition shown in Fig. 13(b) for the VAR material had dimple-rupture with more quasi-cleavage and some evidence of tearing. The ESR material in Fig. 14(b) shows more quasi-cleavage. This difference is mirrored in Fig. 16 which compares fracture toughness of the ESR and VAR material. It

was found that the ESR steel had a slightly lower K_{IC} at 300°C than the VAR steel.

In the 400°C temper condition the VAR steel had a much lower K_{IC} value than the ESR steel. This is shown in Fig. 16 for the transverse orientations. This was probably due to the onset of temper embrittlement in the VAR material. The fracture surfaces showed this effect. Figure 13(c) shows the grain boundary decohesion associated with temper embrittlement at 400°C for the VAR steel. Figure 14(c) contrasts the difference. In the same condition the ESR steel shows a dimple rupture mode of fracture. Above 400°C there is a general recovery of toughness for the VAR steel and this is seen in Figs. 13(d) and 14(d). The fracture surface morphology showed approximately the same mode of fracture for both materials.

These results supported the conclusion that the phosphorous may have segregated to the prior austenite grain boundaries in the VAR material. The ESR process eliminated enough phosphorous such that temper embrittlement was eliminated at this grain size. The explanation for this was as follows: as the grain size increased the surface area decreased so that for a given amount of an impurity, a smaller amount was required to cause embrittlement.

2. <u>The Effect of Variation in Inclusion Contents</u>

As was mentioned above, inclusions act as crack initiators which can lower the toughness if present in higher concentration and a coarser distribution. The inclusion spacing, which is a measure of these two things, has been related to the toughness by Krafft.[23] He found a correlation between the calculated zone size and the measured inclusion

spacing for a high S steel in that the higher sulphur concentration will produce large inclusions and a coarse dispersion which reduced impact energies. It was expected that a modification of the inclusion and/or a reduction in the impurity contents, such as S, would lead to higher impact values. This is seen in Fig. 11. The ESR material which had fewer inclusions also had higher impact energies throughout the tempering sequence. Pellisier[27] reported that there was a difference in toughness for a steel which had decreasing amounts of sulphur from 0.049% to 0.008%. The decrease in sulphur concentration in the present study was not as dramatic but was half from that produced by the VAR process and this would be expected to affect toughness. The slag layer in the ESR process can be adjusted in chemical composition to remove sulphur.[22,29] The reduction in sulphur reduces the inclusion content. The inclusions in the ESR and VAR materials were found to be MnS; however, the ESR steel had significantly fewer inclusions as seen in Fig. 7. The ESR process also caused the inclusions that remained to be in a finer distribution. The metal droplets fall through the impurity-trapping slag and collect in a pool (see Fig. 1). The mold has a slag layer on the wall and is continuously cooled such that porosity and other casting defects are inhibited which results in fewer and finer inclusions. This is also noticed in Fig. 7.

The size and number of inclusions control the longitudinal and transverse mechanical properties, especially toughness.

As mentioned earlier, inclusions form sheets upon rolling. These sheets provide an easy path for crack propagation. The effect of orientation can be seen in Fig. 9 for the VAR material. The K_{IC} values

were very sensitive to orientation particularly between 350 and 500°C. The effect of reducing the inclusion count can be seen in Fig. 10 where the cleaner ESR material showed very little sensitivity to crack orientation. This is further demonstrated in Fig. 11 which shows that the transverse and longitudinal C_v values for the ESR 300-M were nearly equal, whereas those of the VAR steel sometimes exhibited a 10 ft-lb difference.

Hence, the C_v values demonstrate the two effects of reduced inclusion content. The first is that the crack orientation of a cleaner steel is less sensitive to crack propagation. Thus the ESR 300-M, which is a cleaner steel, had equivalent Charpy values in the longitudinal and transverse directions. The second effect which was also observed in the ESR 300-M was that fewer inclusions lead to a higher Charpy value. This investigation has shown that it is possible to improve the mechanical properties of 300-M by employing the electroslag refining process in manufacturing.

V. CONCLUSIONS

1. Electroslag refined 300-M had significantly lower sulphur and phosphorous concentrations than its vacuum arc remelted counterpart.

2. ESR process reduced the size and number of inclusions.

3. MnS inclusions were found in the fracture surface of the VAR 300-M

4. ESR 300-M was found to be much less sensitive to crack or notch orientation than the VAR 300-M. This may be due to the fewer inclusions in the ESR material.

5. ESR 300-M had higher C_v energies than the VAR and this was probably due to the lower sulphur content.

6. ESR 300-M was insensitive to temper embrittlement due to its lower phosphorous concentration.

ACKNOWLEDGEMENTS

The author wishes to gratefully extend his thanks and appreciation to Professors Earl Parker and Victor Zackay for their continued guidance and support throughout this investigation. He would also like to thank the staff and students at MMRD and friends, particularly Dr. M. S. Bhat, for helpful discussion and for carefully reviewing the manuscript. Also to be thanked are Ramesh and Naresh Kar, Ana Maria Llopis, Larry Thompson, Peter Ilyin, Bill Peterson, and John Anderson for the friendship and encouragement essential to a graduate career.

This work was done with support from the U. S. Energy Research and Development Administration through the Materials and Molecular Research Division of the Lawrence Berkeley Laboratory.

REFERENCES

1. ASM STP-370, p. 1.
2. Lloyd, G. T. Owen, and L. Baker, J. of Australian Inst. Metals 16, 1 (1971).
3. Kay, D., A. Mitchell and M. Ram, JISI 208(1), 121 (1970).
4. Wahlster, M. and A. Choudhury, Metals Prog. 95(4), 107 (1969).
5. Cooper, C. and D. Kay, JISI, 856, Sept. 1970.
6. Williams, A., JISI, 581, July 1964.
7. Robinson, W. and J. Grainger, Metallurgia 67, 161 (1963).
8. Huang. D. and G. Thomas, Met Trans. 2, 1587 (1971).
9. Das, S. and G. Thomas, ASM 62, 659 (1969).
10. Wood, W., R. Clark, V. Zackay and E. Parker, Met. Trans. 5, 1663 (1974).
11. Thomas, G., LBL-4703 (1974), Lawrence Berkeley Laboratory, Berkeley, California.
12. Parker, E. and V. Zackay, Engr. Fracture Mech. 7, 371 (1975).
13. Clark, G., R. Ritchie and J. Knott, Nat. Phys. Sci. 239(94), 104 (1972).
14. Ritchie, R. and J. Knott, Met. Trans. 5, 782 (1974).
15. Rao, B., M. S. Thesis, LBL-3794 (1975), Lawrence Berkeley Laboratory, Berkeley, California.
16. Mitchell, A. and M. Etieene, Trans. Met. Soc. AIME 242, 1462 (1968).
17. Fredriksson, H. and O. Jarleborg, J. of Metals, 32 (1972).
18. Mitchell, A. and S. Joshi, Met. Trans. 4, 631 (1973).
19. Mitchell, A. and S. Joshi, Met. Trans. 2, 449 (1971).
20. Johnson, A. and A. Hellawell, Met. Trans. 3, 1016 (1973).

21. Horn, R., Ph. D. Thesis, LBL-5787 (1976), Lawrence Berkeley Laboratory, Berkeley, California.

22. Wood, W., Ph. D. Thesis, LBL-1474 (1974), Lawrence Berkeley Laboratory, Berkeley, California.

23. ASTM Std. Specification E399-72.

24. Ritchie, R., unpublished research, Lawrence Berkeley Laboratory, Berkeley, California.

25. Miller, J., Trans. ASTM 57, 892 (1964).

26. deMiramon, B., M. S. Thesis, UCRL-17849 (1967).

27. Phillesier, G., Engr. Fract. Mech. 1, 55 (1968).

28. Feige, N. and T. Murphy, Metals Engr. Q. 7, 53 (1967).

29. Hidge, J., R. Grazier, and F. Boulger, Trans. AIME 215(5), 745 (1959).

30. Knott, J., Fundamentals of Fracture Mechanics, J. Wiley and Sons, N. Y. (1973), p. 214.

31. Ristaini, P. and C. McMahon, Trans. ASM 60, 691 (1967).

32. Irvine, K. JISI 200, 820 (1962).

33. Woodfine, B., JISI 173, 229 (1953).

34. Bhat, M. S., Ph. D. Thesis, LBL-6046 (1977), Lawrence Berkeley Laboratory, Berkeley, California.

Table 1. Chemical Composition of the Electroslag Refined and Vacuum Arc Remelt 300-M Steel

	C	Cr	Mn	Mo	Ni	Si	V	P	S	O
VAR 300M	0.41	0.75	0.84	0.42	1.78	1.62	0.09	0.012	0.002	0.002
ESR 300M	0.40	0.81	0.75	0.37	1.90	1.57	0.11	0.006	0.001	0.008

Table 2. The Longitudinal Tensile Properties of ESR and VAR 300-M

Temper. (°C)	UTS (ksi)	Tield Strength (ksi)	% Red Area	% Elongation
ESR†				
AQ	323.2	264.9	5	-
200	307	240.3	38	11.4
300	289.3	236.3	45	12.8
400	271.4	237.8	48	13.1
500	242.5	200.3	46	18.3
600	212.7	195.8	47	21.2
VAR				
AQ	358*	218*	11*	-
200	304	238	41	13.6
300	292	250	47	12.0
400	274	245	48	13.0
500	230	202	36	12.8
600	188	170	42	12.5

†3 tests - round tensile

*Ritchie

Table 3. The Longitudinal and Transverse Fracture Toughness

Temper. (°C)	Longitudinal K_{Ic}* (ksi-in$^{1/2}$)	Transverse K_{Ic}* (ksi-in$^{1/2}$)
ESR		
AQ	28.6	29.6
200	45.2	40.7
300	50.1	55.0
400	58.3	54.3
500	66.2	64.3
600	96.6	90.0
VAR		
AQ	31.0	31.9
200	57.5	49.7
300	59	60.9
400	55	47.7
500	62	60.0
600	89†	91.0

*Average three tests

†KQ (apparent); 2 tests invalid

Table 4. The Charpy Impact Energy of ESR and VAR 300-M

Temper. (°C)	Longitudinal* C_v	Transverse* C_v
ESR		
AQ	15.0	13.5
200	20.25	20.0
300	19.0	19.5
400	18.0	18.25
500	12.5	13.0
600	16.5	16.5
VAR		
AQ	12	7.0
200	18	9.0
300	15.5	8.75
400	14.5	7.5
500	7.0	6.5
600	12.0	7.0

*3 tests

FIGURE CAPTIONS

Fig. 1. Schematic of the electroslag refining process.

Fig. 2. (a) Schematic of specimen orientation in the forged and rolled plate. (b) Photograph of vertical tube furnace with argon cylinder used for heat treatment of specimens.

Fig. 3. Sketch of compact tension specimen.

Fig. 4. Sketch of round tensile specimen.

Fig. 5. Sketch of Charpy impact specimen.

Fig. 6. Optical photomicrographs comparing the microstructure of the (a) VAR 300-M and (b) ESR 300-M in the as-received condition.

Fig. 7. Optical photomicrographs of (a) ESR 300-M and (b) VAR 300M after an austenitization of 1 hr at 900°C with an oil quench. These were polished to 1μ.

Fig. 8. Plot of the elongation and reduction in area of the ESR and VAR 300-M.

Fig. 9. Plot of plane strain fracture toughness (K_{IC}) and tempering temperature for the longitudinal and transverse orientation of the VAR 300-M.

Fig. 10. Plot of the plane strain fracture toughness and tempering temperature for the longitudinal and transverse orientations of the ESR +300-M.

Fig. 11. Plot of the Charpy impact energy and tempering temperatures for the transverse and longitudinal orientations of the ESR and VAR 300-M.

Fig. 12. A plot of the percent retained austenite and tempering temperature for the ESR 300-M.

Fig. 13. Fracture surfaces of the VAR 300-M after austenitization at 900°C for 1 hr, oil quench for (a) as-quenched, (b) 300°C temperature, (c) 400°C temperature, and (d) 500°C temperature. AC in (a) shows an inclusion trail.

Fig. 14. Fracture surfaces for the ESR 300-M after austenitization at 900°C for 1 hr, oil quench for the temperature conditions of (a) as-quenched, (b) 300°C, (c) 400°C, and (d) 500°C.

Fig. 15. Optical photomicrographs of the ESR 300-M after austenitization at 900°C for 1 hr in the temperature conditions of (a) as-quenched, (b) 300°C, (c) 400°C, and (d) 500°C.

Fig. 16. Plot of plane strain fracture toughness, K_{IC}, for the ESR and VAR 300-M materials in the transverse orientations.

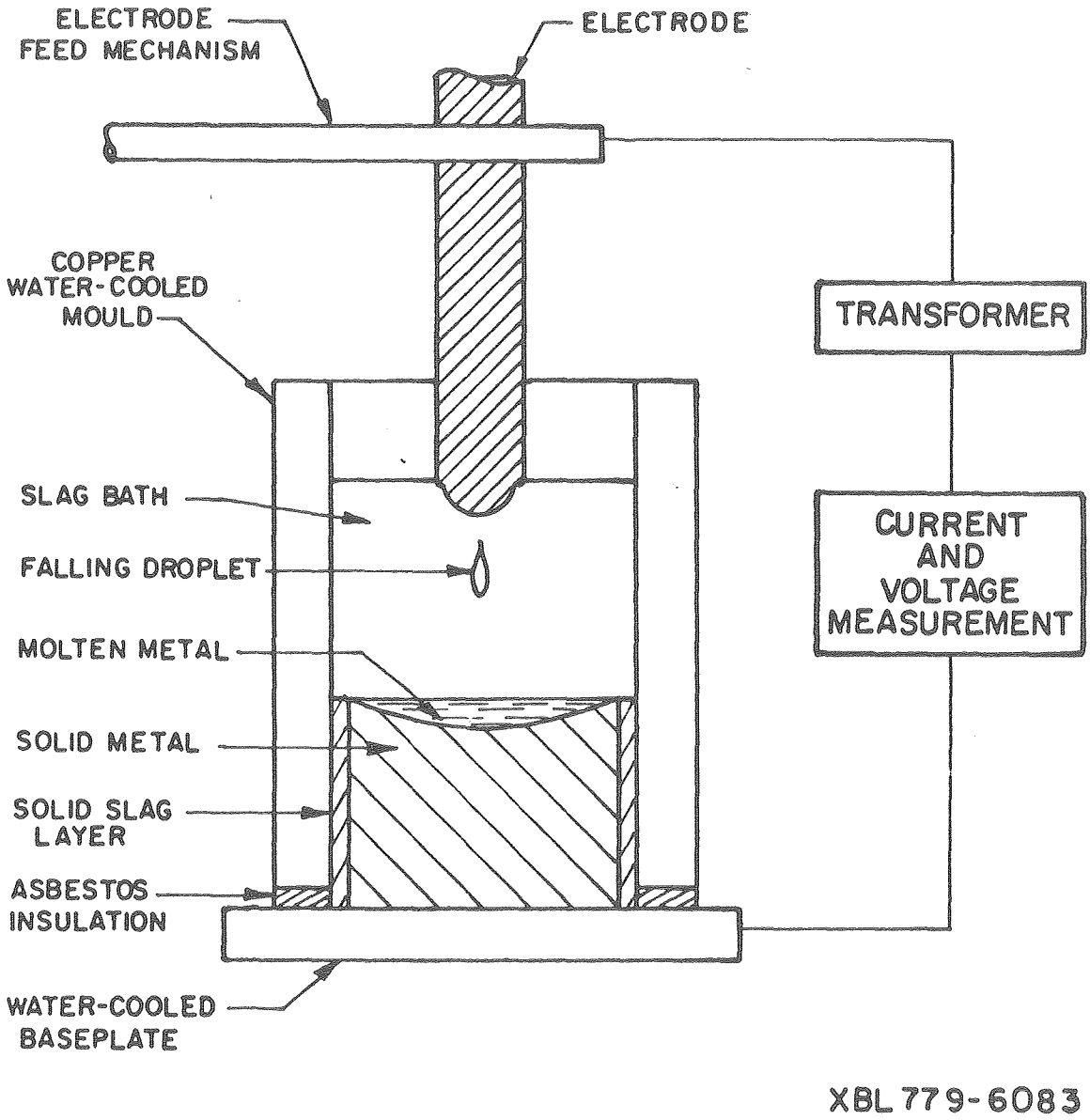
ELECTRODE FEED MECHANISM
ELECTRODE
COPPER WATER-COOLED MOULD
TRANSFORMER
SLAG BATH
FALLING DROPLET
CURRENT AND VOLTAGE MEASUREMENT
MOLTEN METAL
SOLID METAL
SOLID SLAG LAYER
ASBESTOS INSULATION
WATER-COOLED BASEPLATE
XBL 779-6083

Fig. 1

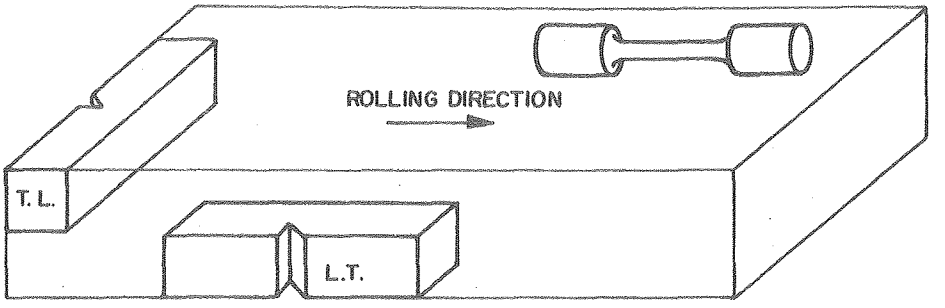

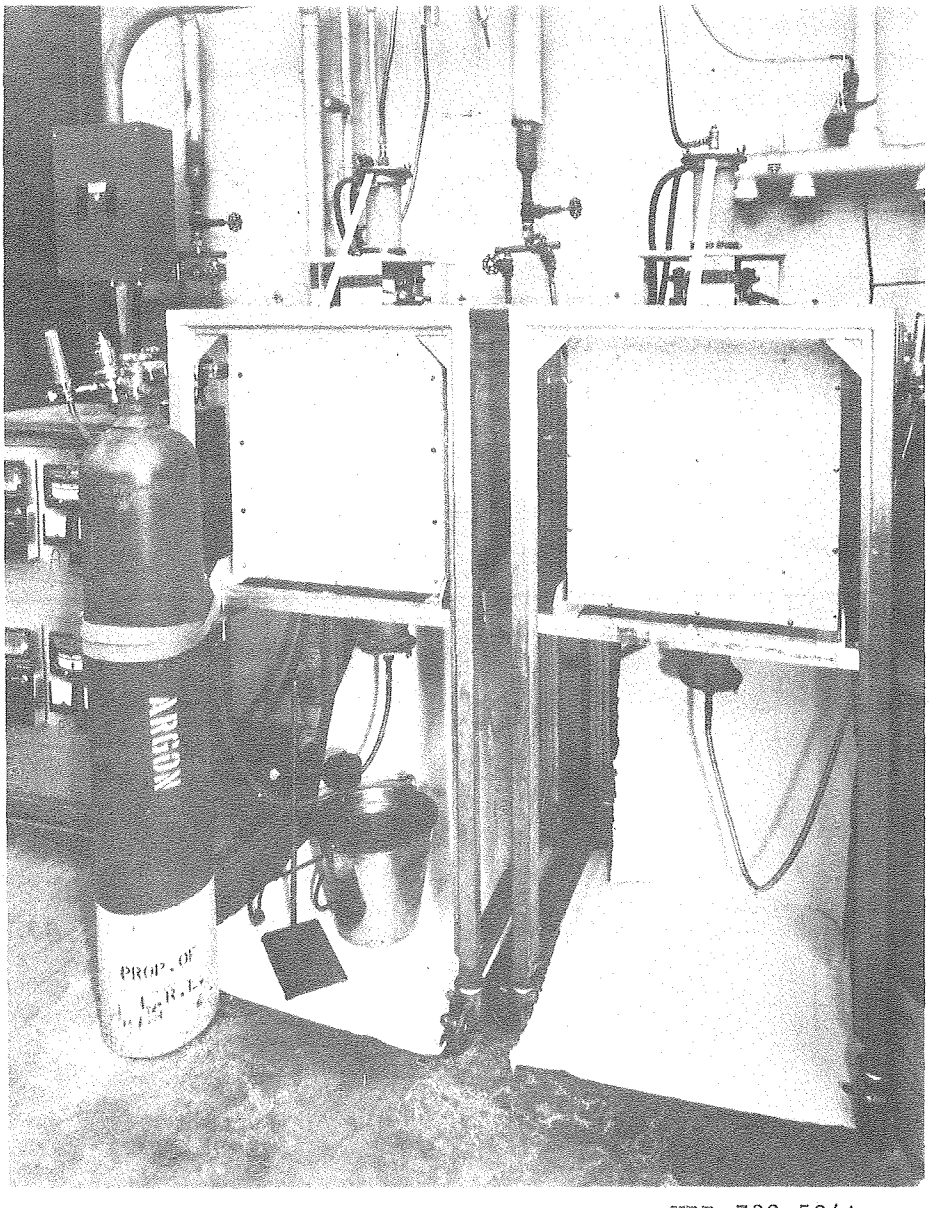

XBB 732-504A

Fig. 2

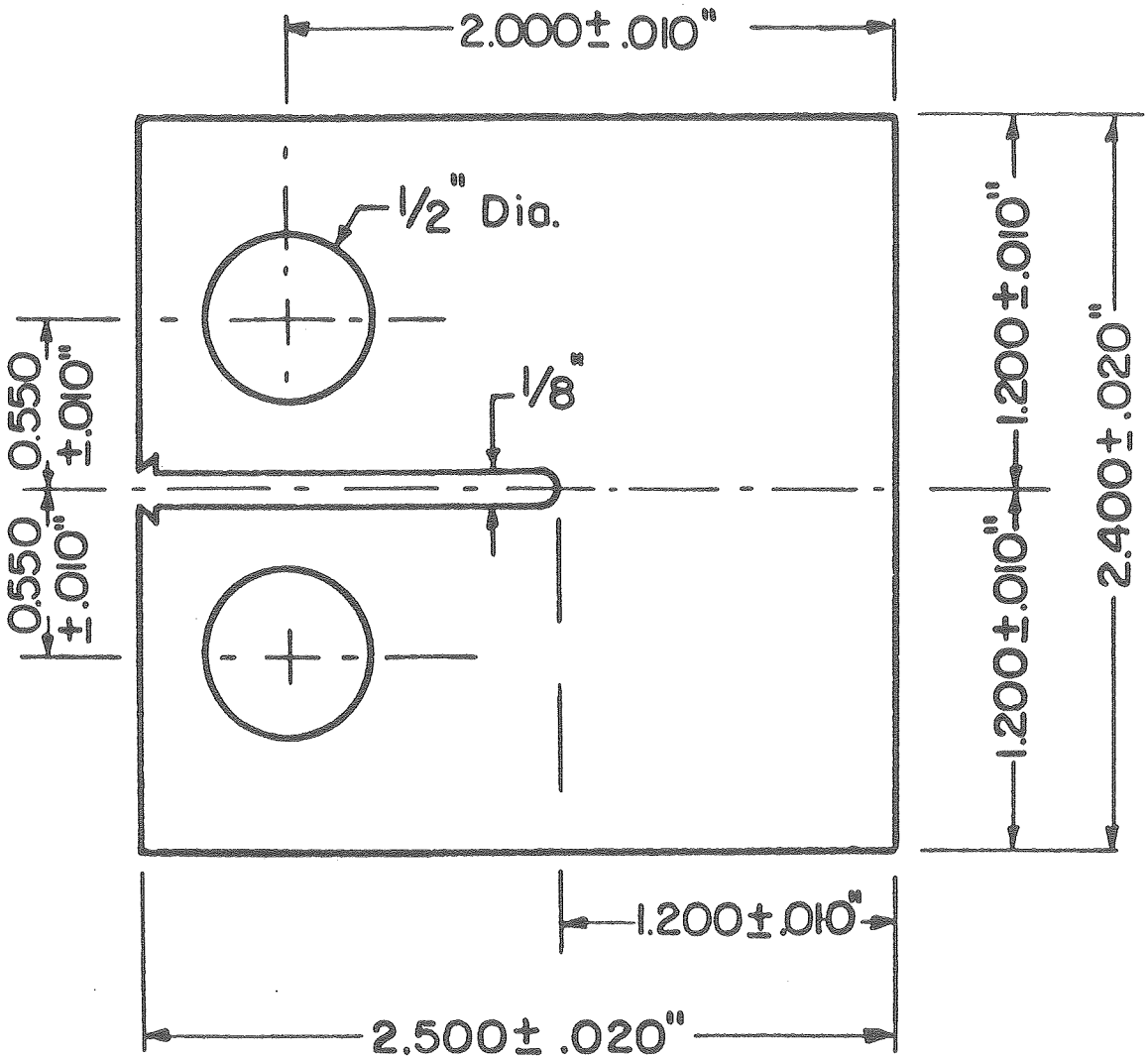

XBL 7612-10410C

Fig. 3

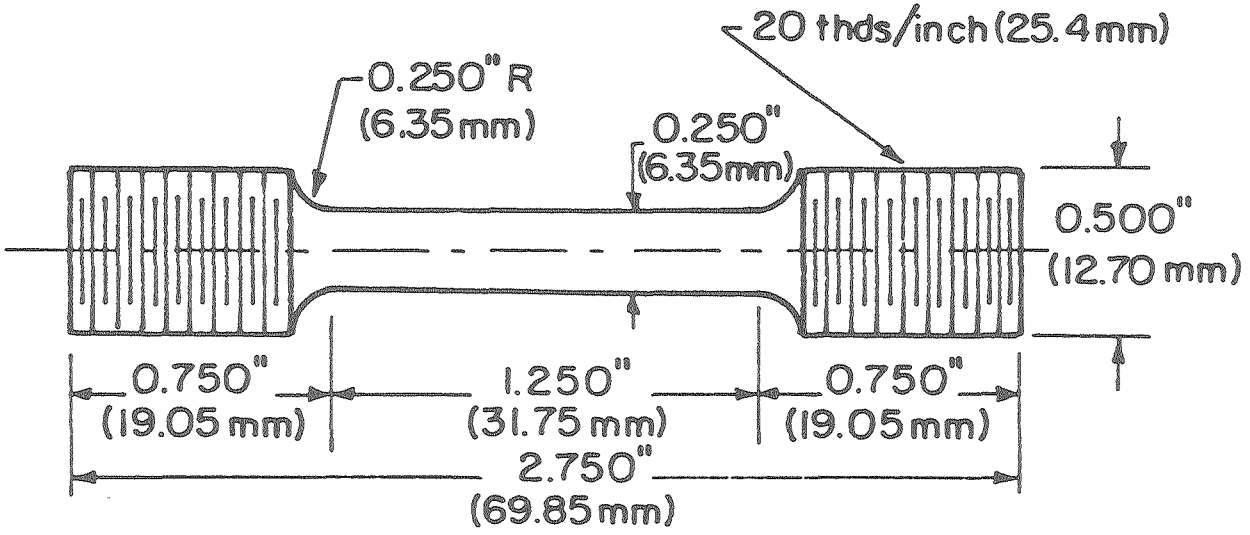

XBL 736-6280B

Fig. 4

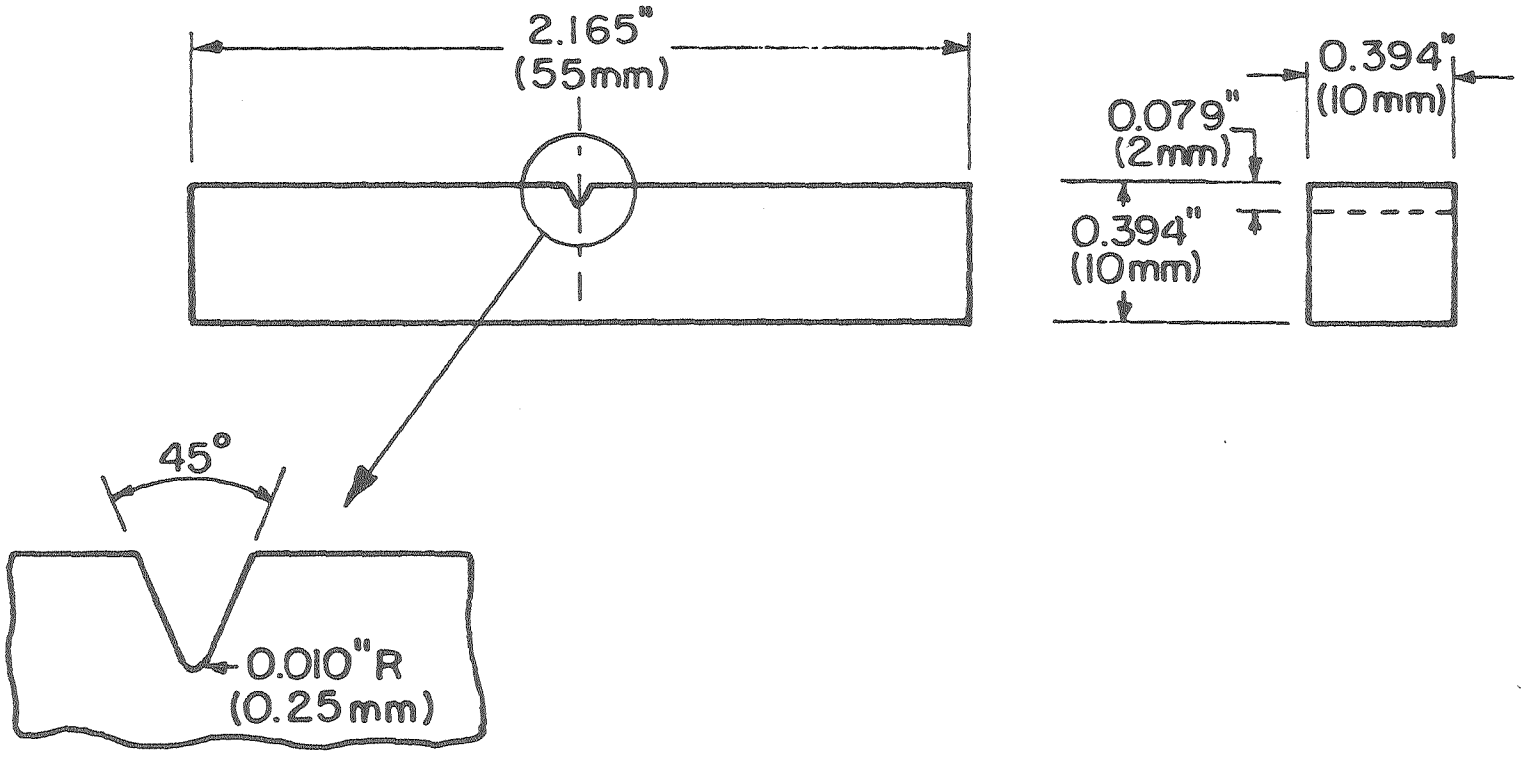

XBL 736-6280A

Fig. 5

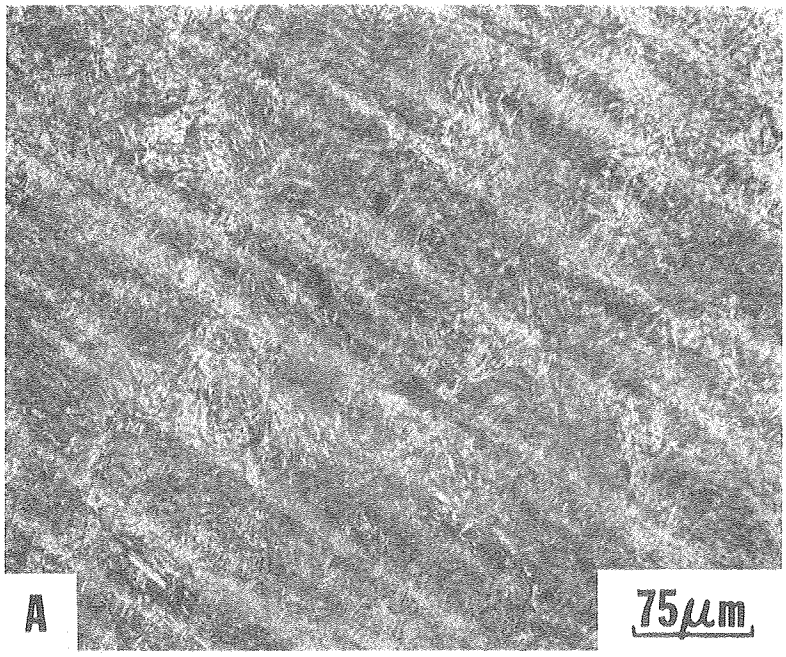

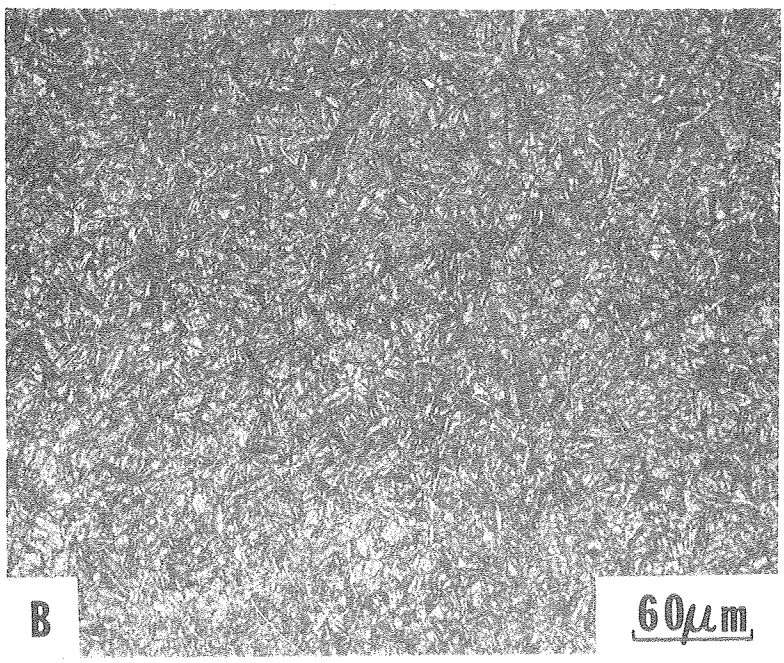

XBB 779-9120

Fig. 6

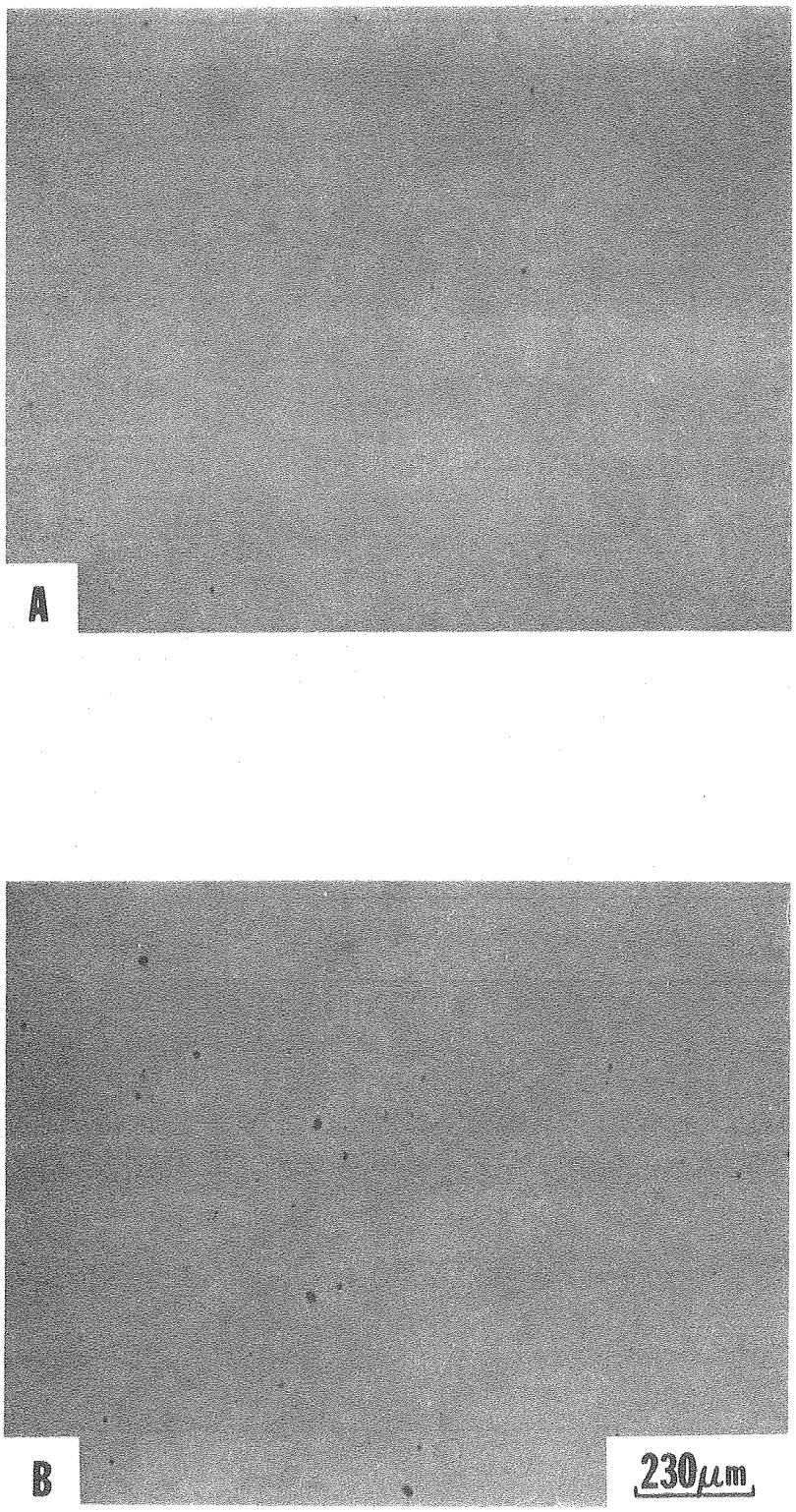

XBB 779-9118

Fig. 7

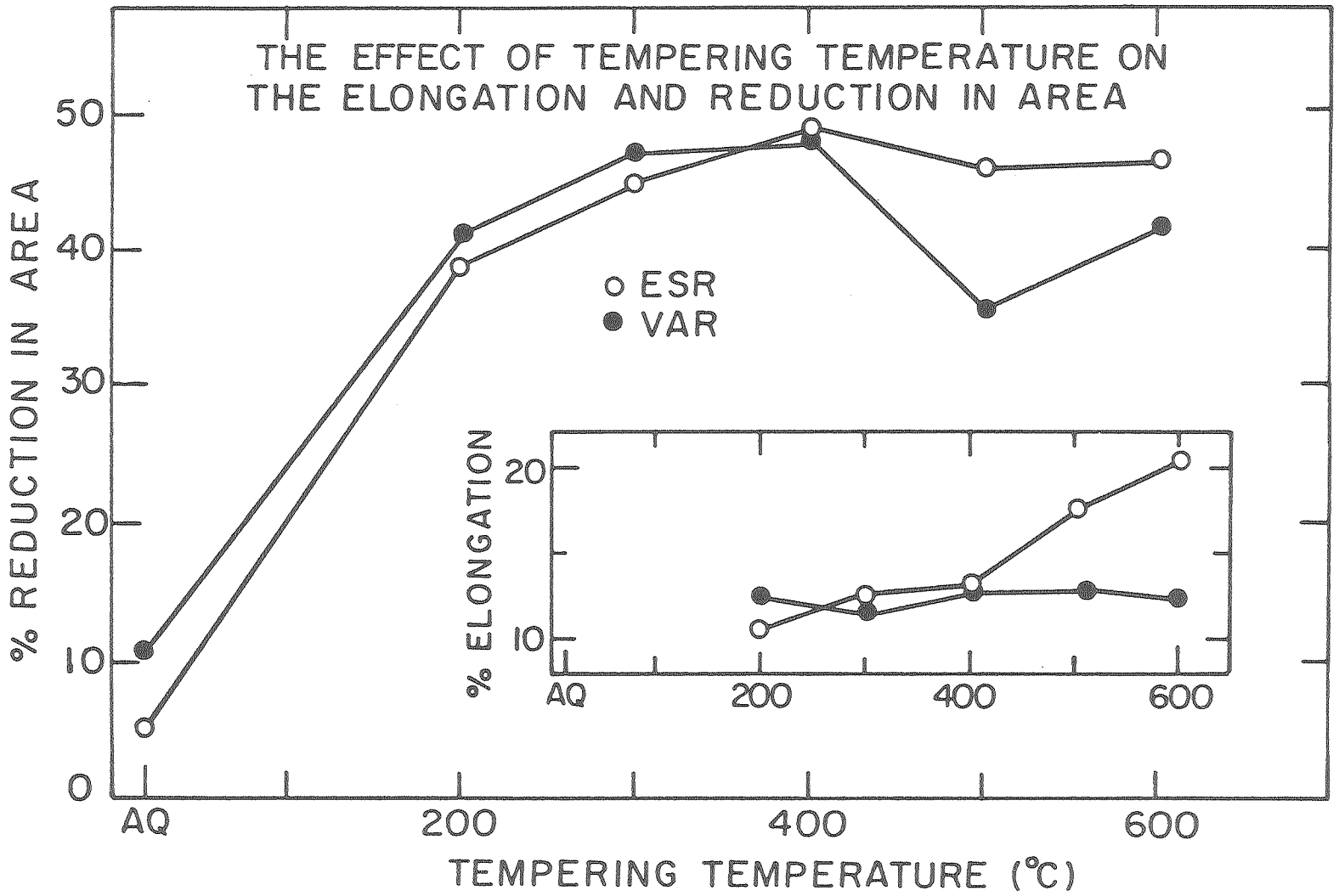

XBL 779-6076

Fig. 8

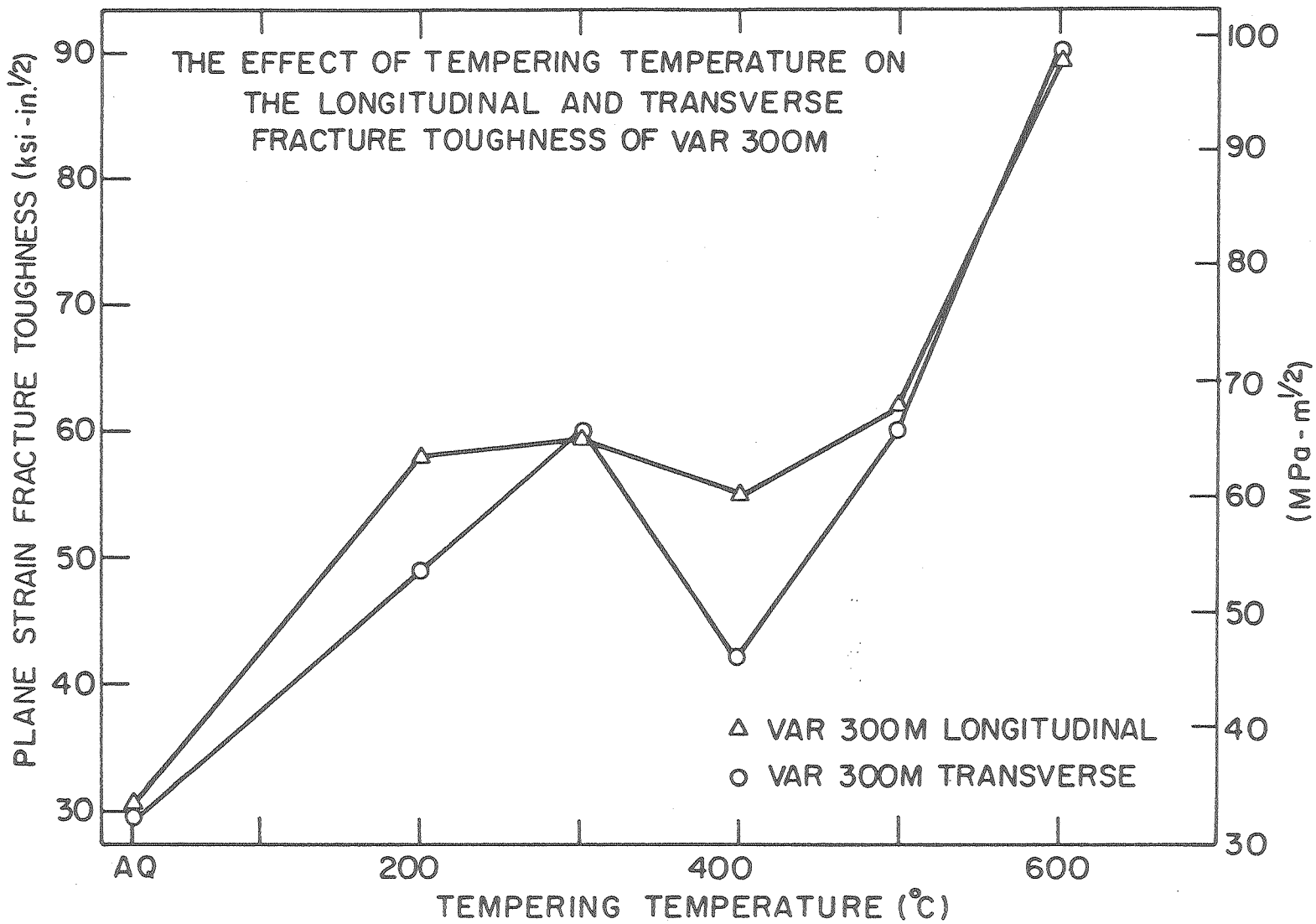

XBL 779-6078

Fig. 9

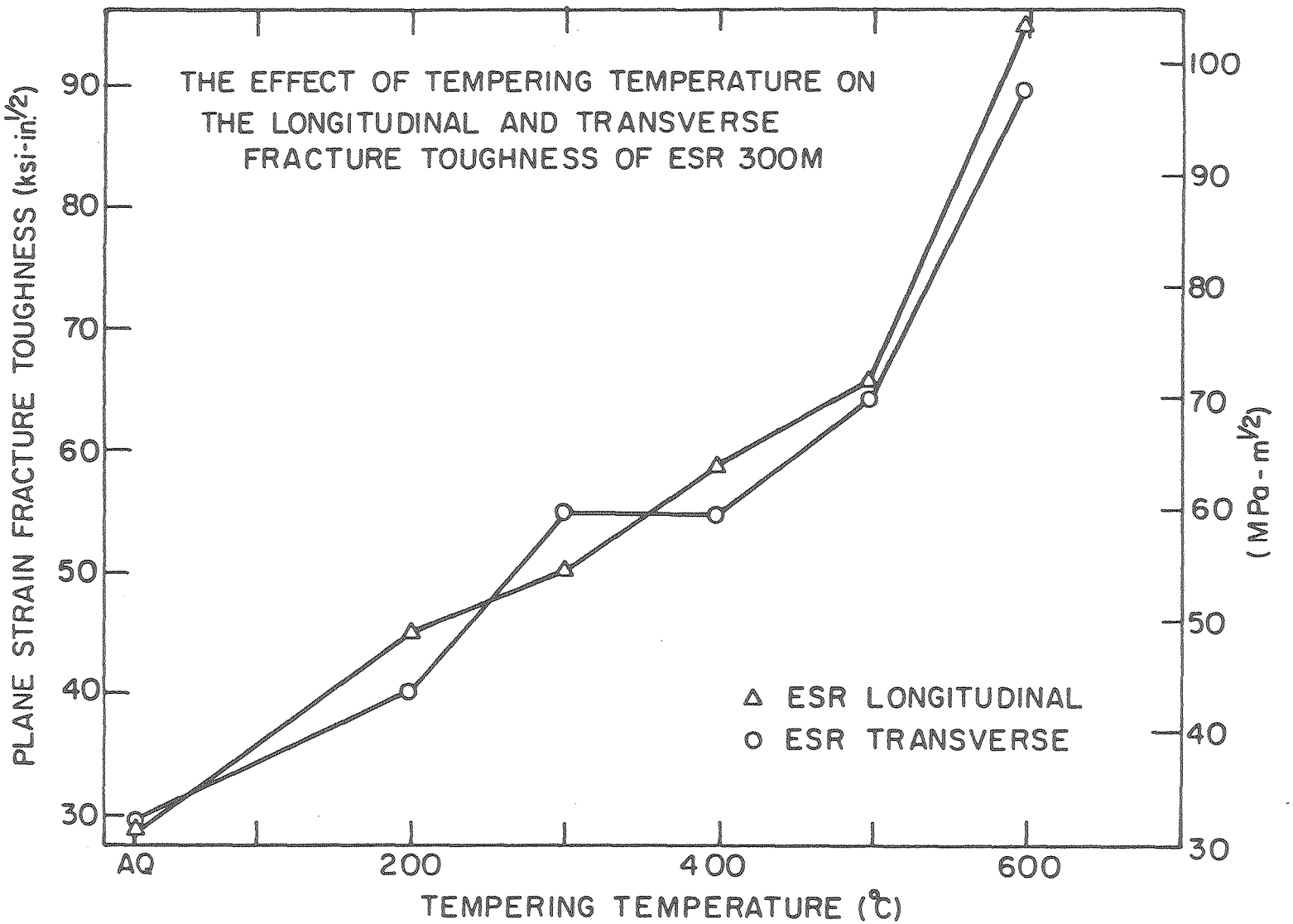

Fig. 10

XBL 779-6077

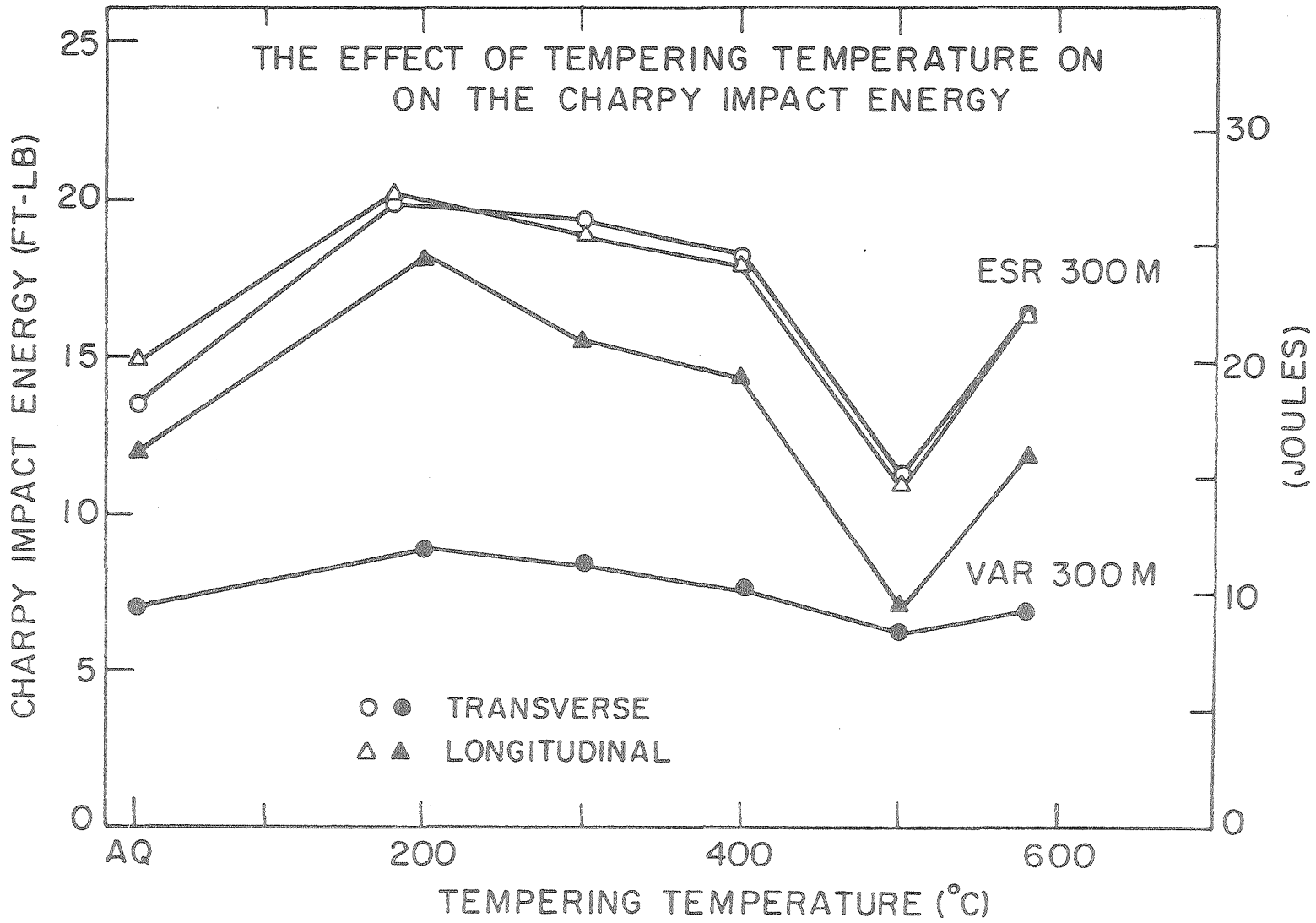

Fig. 11

XBL 779-6075

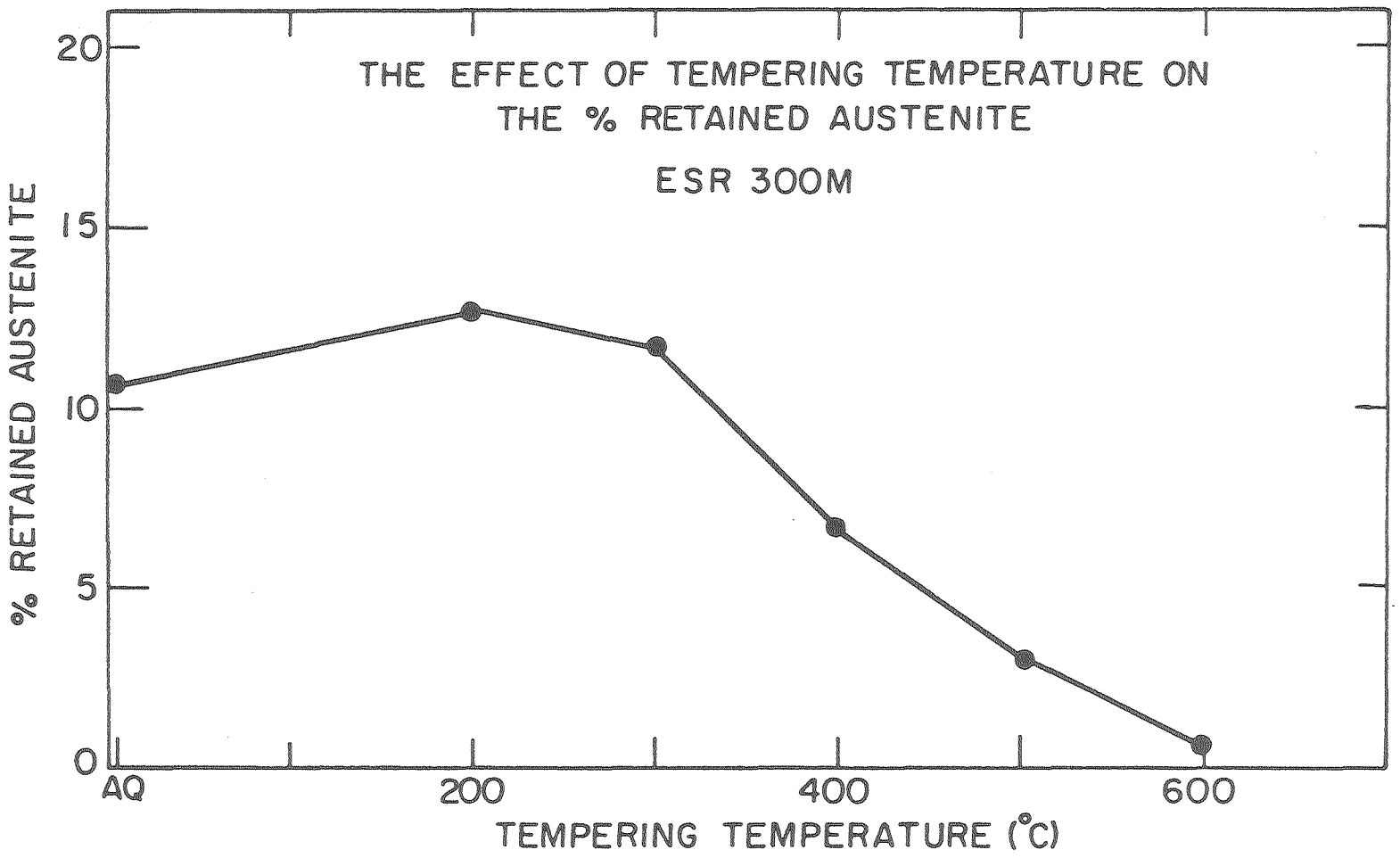

XBL 779-6080

Fig. 12

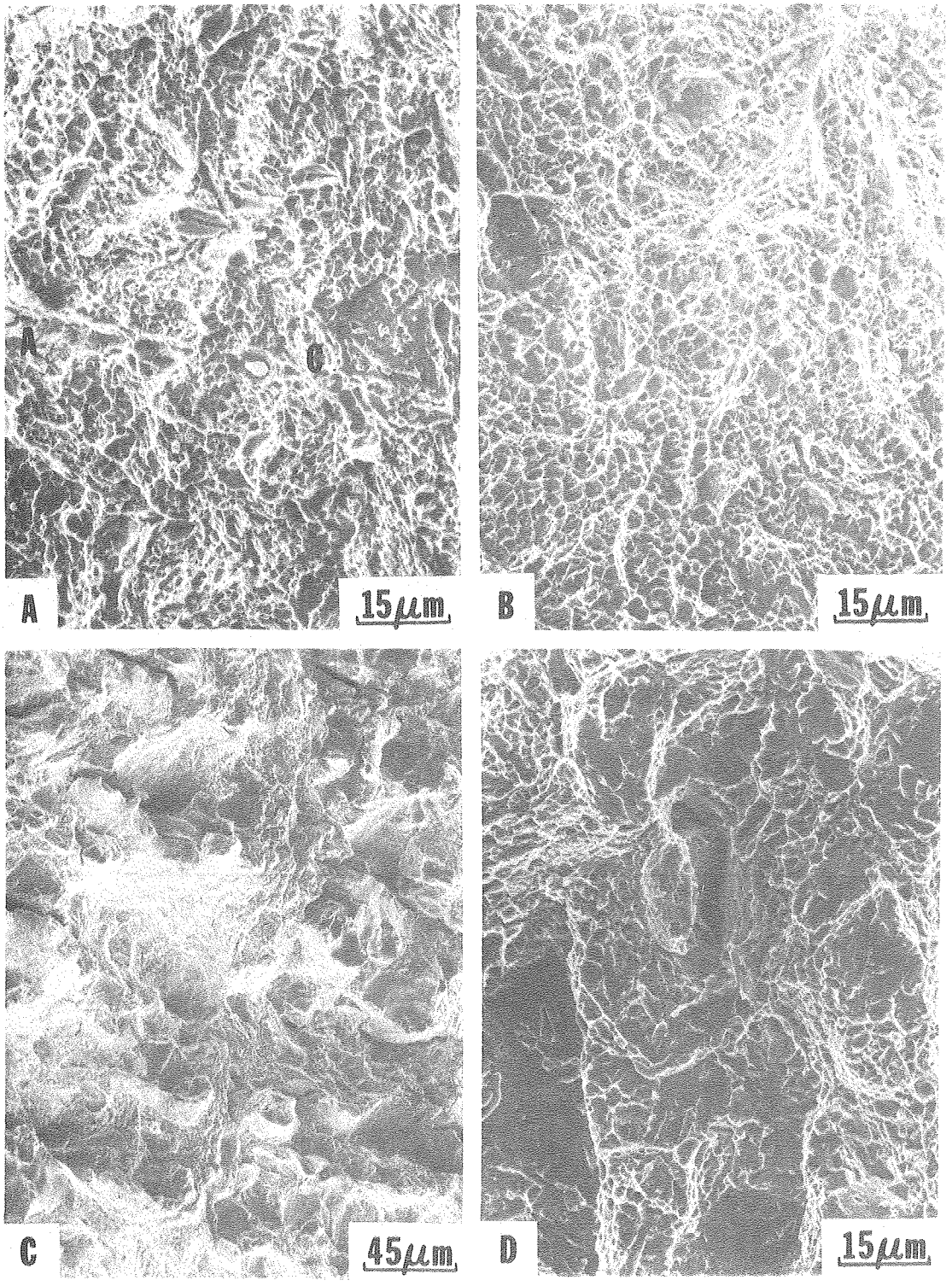

XBB 779-9121

Fig. 13

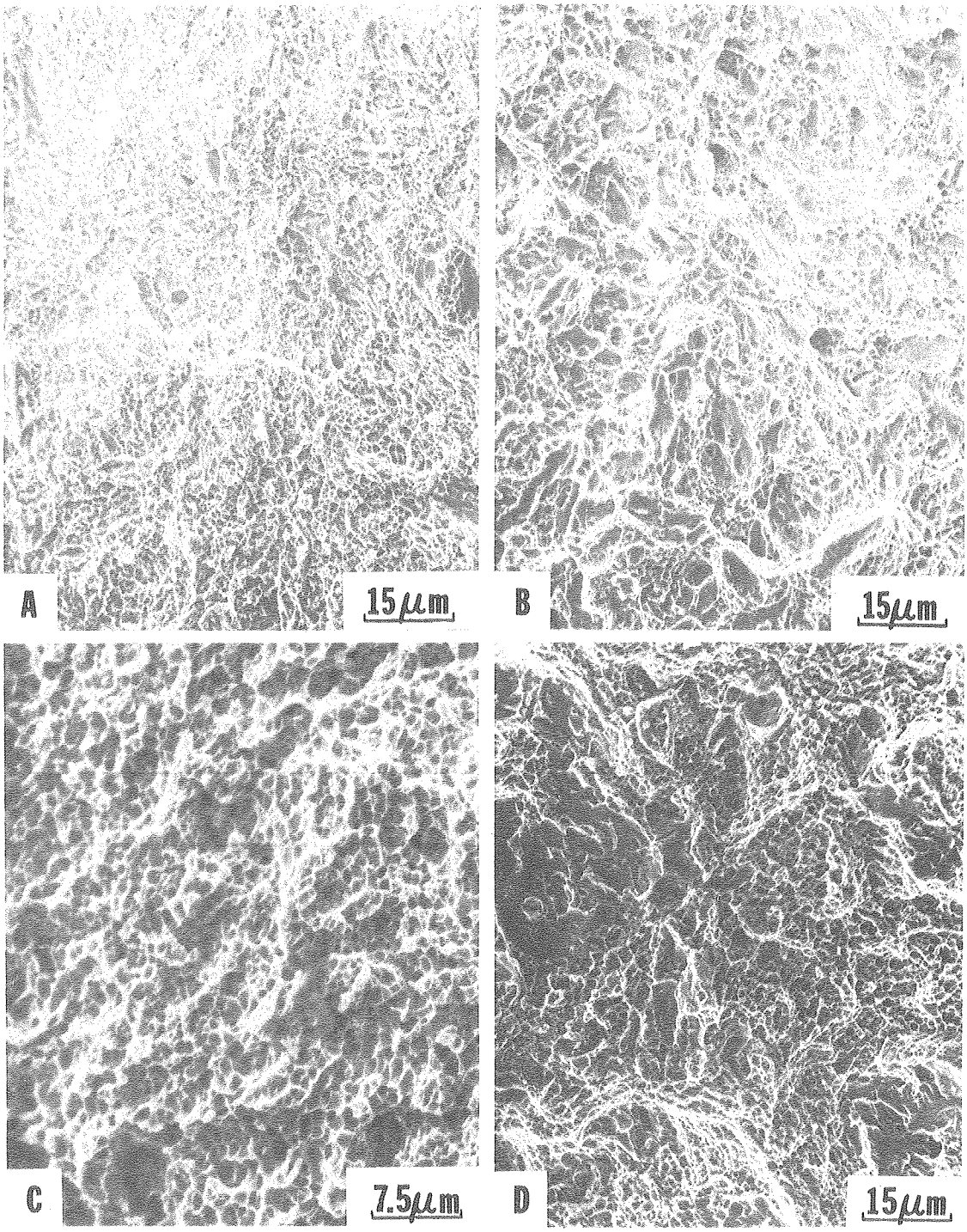

XBB 779-9119

Fig. 14

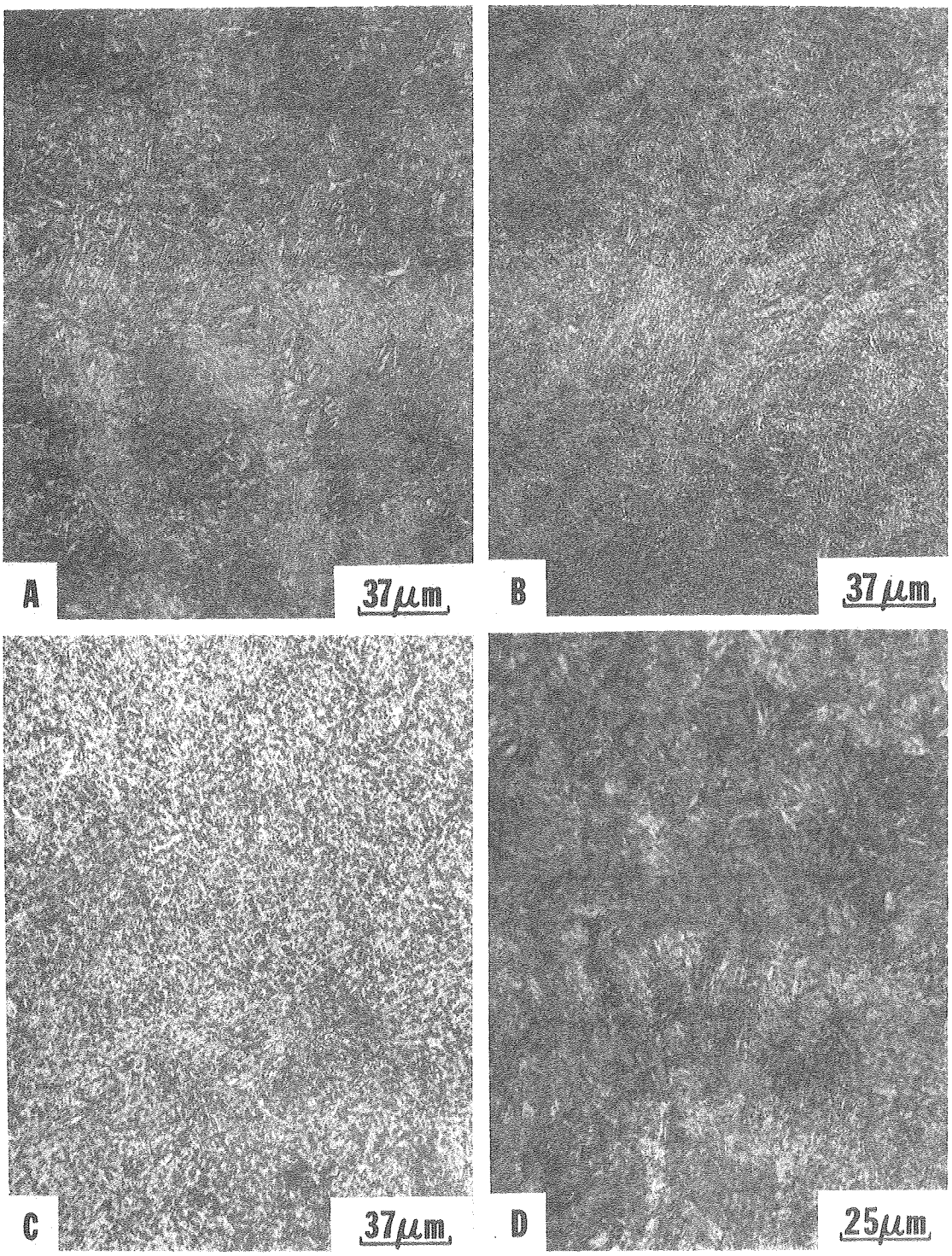

XBB 779-9122

Fig. 15

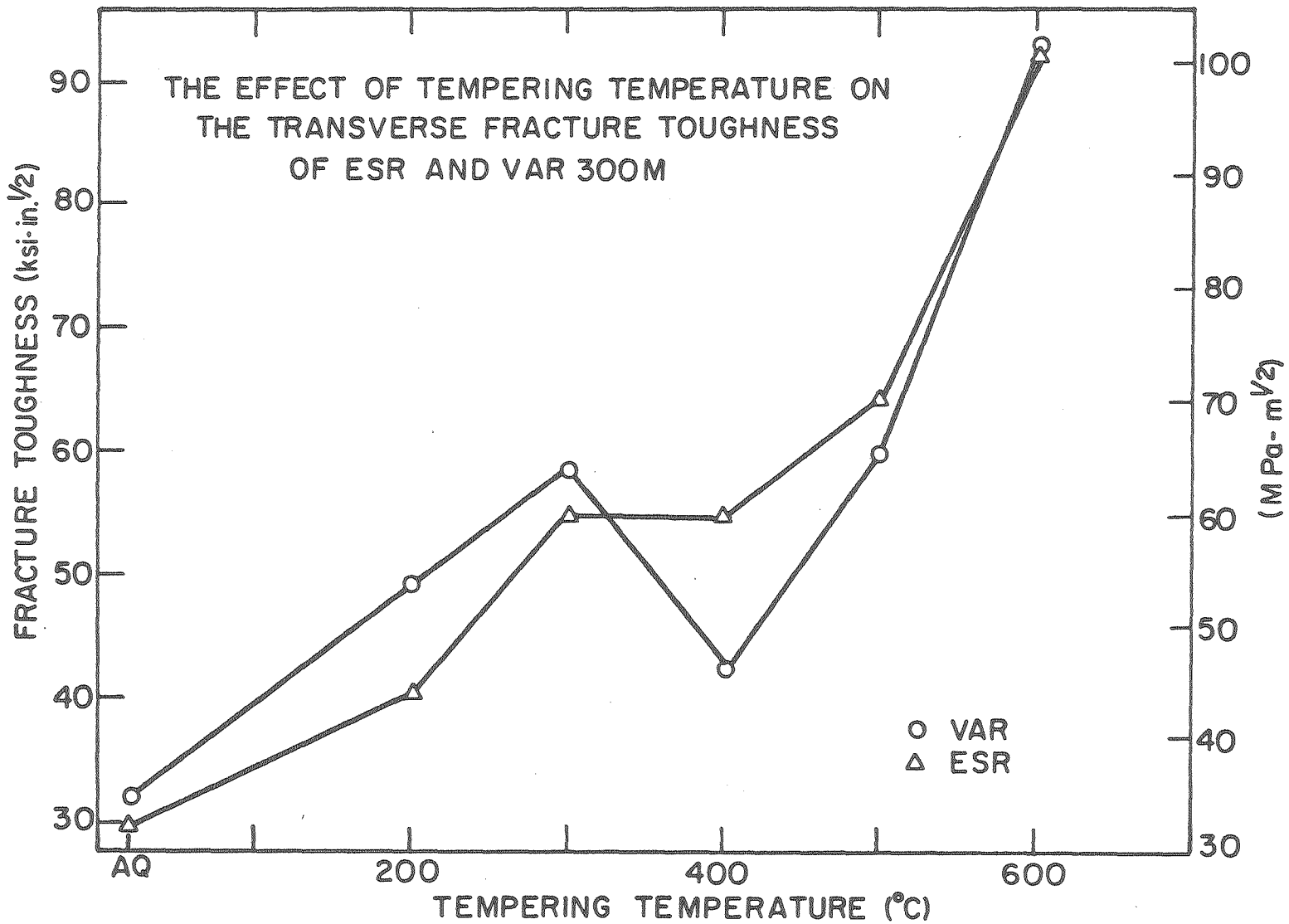

XBL 779-6079

Fig. 16

This report was done with support from the Department of Energy. Any conclusions or opinions expressed in this report represent solely those of the author(s) and not necessarily those of The Regents of the University of California, the Lawrence Berkeley Laboratory or the Department of Energy.

TECHNICAL INFORMATION DEPARTMENT
LAWRENCE BERKELEY LABORATORY
UNIVERSITY OF CALIFORNIA
BERKELEY, CALIFORNIA 94720